



INTERNATIONAL JOURNAL OF ENGINEERING SCIENCES & RESEARCH TECHNOLOGY

EXPERIMENTAL ANALYSIS OF CORRUGATED FLATE PLATE COLLECTOR FOR EFFLUENT EVAPORATION

Deepak Sonawane*, Manisha Magare, Ramdas Patthe

Research Scholar Mechanical Engineering Department, SGGSIET, Nanded, India

M.Tech Student Mechanical Engineering Department, SGGSIET, Nanded, India

Research Scholar Mechanical Engineering Department, SGGSIET, Nanded, India

ABSTRACT

Many industrial processes produce effluents also termed as waste water which can cause damage to environment if not treated properly. Evaporation of water content of effluent results in reducing quantity of the stuff and also increases its concentration. As the quantity of effluent is reduced it becomes easier to treat or dispose off in smaller area. Conventionally such effluent is dried naturally in the ponds with Sun and the Wind. In few cases the evaporation is accelerated with use of external heating sources as well as using fans and blowers to create air movement and agitation. Use of aerators or sprays is also employed for increasing surface area of the effluent which aids in evaporation. All such measures consume extra auxiliary power. So, it is essential to increase aperture area by using corrugated flat plate collector which will overcome all these problems, will have higher rate of evaporation and disposal of effluent.

KEYWORDS: *Corrugated flat plate collector, Effluent, Evaporation, Solar Energy.*

INTRODUCTION

Theory of Evaporation

For molecules of a liquid to evaporate, they must be located near the surface, be moving in the proper direction, and have sufficient kinetic energy to overcome liquid-phase intermolecular forces. When only a small proportion of the molecules meet these criteria, the rate of evaporation is low. Since the kinetic energy of a molecule is proportional to its temperature, evaporation proceeds more quickly at higher temperatures. As the faster-moving molecules escape, the remaining molecules have lower average kinetic energy, and the temperature of the liquid decreases. This phenomenon is also called evaporative cooling. This is why evaporating sweat cools the human body. Evaporation also tends to proceed more quickly with higher flow rates between the gaseous and liquid phase and in liquids with higher vapour pressure. For example, laundry on a clothes line will dry (by evaporation) more rapidly on a windy day than on a still day. Three key parts to evaporation are heat, atmospheric pressure (determines the percent humidity) and air movement.

On a molecular level, there is no strict boundary between the liquid state and the vapour state. Instead, there is a Knudsen layer, where the phase is undetermined. Because this layer is only a few molecules thick, at a macroscopic scale a clear phase transition interface can be seen.

Liquids that do not evaporate visibly at a given temperature in a given gas (e.g., cooking oil at room temperature) have molecules that do not tend to transfer energy to each other in a pattern sufficient to frequently give a molecule the heat energy necessary to turn into vapour. However, these liquids are evaporating. It is just that the process is much slower and thus significantly less visible.

Solar effluent evaporation system

Industries during the manufacturing process generate huge quantity of high toxic effluents. The main objective of effluent treatment plants is to process the effluent discharge and bring it below pollution control norms. There are many types of effluent treatments done in the industry. Evaporative treatment process is one of major type that is used worldwide. It mainly includes evaporation in multiple effect evaporator, drying of concentrate, separation of solids by centrifuging / decanting, drying of wet solids to convert into powder. Process separates entire effluent into water and dry solids. Water can be recycled in the plant and solids are either reused as a product or incinerated for generation of heat or disposed as solid effluent depending upon its properties. The evaporation process is driven by

heat transferred from hot steam to a solution at a lower temperature across a metallic heat transfer surface. The absorbed heat causes vaporization of the solvent, usually water, and an increase in the solute concentration. The resulting vapour may be vented to the atmosphere, or condensed for reuse.

As the main energy requirement is in the form of heat, typically in the temperature range of 100 to 120°C. The solar thermal flat plate collector system can easily supply heat in this temperature range using either steam or pressurized hot water

Theoretical Analysis

The following analysis an approximate equation is deduced that predicts the convective mass transfer or evaporation rate per unit area from a horizontal water surface exposed to the natural environment. Initially the transfer rate due to natural convection only is deduced and the equation is then extended to make provision for windy (forced convection) conditions. Consider a stationary semi-infinite fluid (binary mixture consisting of air and water vapor) in which the concentration, of the species of interest (water vapor) is initially uniform. Beginning with the time $t = 0$, the concentration at the $z=0$ boundary or surface is maintained at a greater level C_{vo} as shown in figure 1(a). Water vapor will diffuse into the semi-infinite medium to form a concentration boundary layer, the thickness of which increases with time.

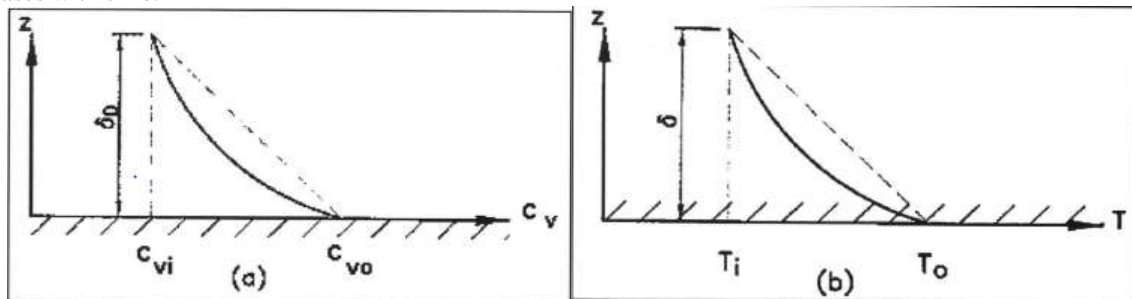


Figure 1. Concentrations Or Temperature Distribution In Semi-Infinite Medium

The mathematical equation of time dependent diffusion in a binary mixture, expressed in terms of the molar concentration c is as follows:

$$D \frac{\partial^2 c}{\partial z^2} = \frac{\partial c}{\partial t} \dots (1)$$

The diffusion flux is driven solely by the concentration gradient strictly in an isothermal and isobaric medium. Nevertheless, equation 1 is a good approximation in many non-isothermal systems, where temperature differences are relatively small. If changes in Kelvin temperature are small the diffusion coefficient D can be assumed to be constant. Equation 1 is analogous to the time-dependent equation for heat conduction into a semi-infinite solid body i.e.

$$\alpha \frac{\partial^2 T}{\partial z^2} = \frac{\partial T}{\partial t} \dots (2)$$

If the temperature of a semi-infinite solid is initially uniform at T_i and a sudden increase in temperature to T_o occurs at $z = 0$ as shown in figure 1(b), Schneider shows that the

Temperature gradient at $z = 0$ is given by q_t

$$\frac{\partial T}{\partial z} = \frac{T_i - T_o}{(\pi \alpha t)^{1/2}} \dots (3)$$

The corresponding heat flux is

$$q_t = -k \frac{\partial T}{\partial z} = \frac{k(T_o - T_i)}{(\pi \alpha t)^{1/2}} \dots (4)$$

An effective heat transfer coefficient can be expressed in terms of this heat flux i.e.

$$h_t = \frac{q_t}{T_o - T_i} = \frac{k}{(\pi \alpha t)^{1/2}} \dots (5)$$

Similarly, by solving equation 2 for the case where the semi-infinite solid at an initial uniform temperature T_i is suddenly exposed to a constant surface heat flux q_q , the latter can, according to Holman, be expressed in terms of an effective surface temperature T_{oq} as

$$q_q = \frac{k(T_{oq} - T_i)}{\left[2 \left(\frac{\alpha t}{\pi} \right)^{1/2} \right]} \dots (6)$$

The corresponding effective heat transfer coefficient is defined as

$$q_{qt} = \frac{k}{\left[2\left(\frac{\alpha t}{\pi}\right)^{1/2}\right]} = \frac{q_q}{(T_{oq}-T_i)} \dots\dots(7)$$

It follows from equations 5 and 7 that for the same temperature difference i.e. for

$$(T_i - T_o) = (T_{oq} - T_i) \dots\dots(8)$$

$$\frac{h_{qt}}{h_{Tt}} = \frac{\pi}{2} = \frac{h_q}{h_T}$$

Although equation 2 is applicable to a solid, it is a good approximation when applied to a thin layer of gas or vapor near a solid surface. Due to the analogy between mass and heat transfer the solution of equation 1 gives the following relations corresponding to equations 3 to 8 respectively: If the initial concentration at $z = 0$ is suddenly increased to c_{vo}

$$\frac{\partial c_v}{\partial z} = \frac{(c_{vi}-c_{vo})}{(\pi Dt)^{1/2}} \dots\dots(9)$$

The corresponding vapour mass flux is

$$m_v = -D \frac{\partial c}{\partial z} = \frac{(c_{vo}-c_{vi})}{\left[\frac{D}{(\pi t)}\right]^{1/2}} \dots(10)$$

An effective mass transfer coefficient can be expressed in terms of this vapor mass flux i.e.

$$h_{Dt} = \frac{m_v}{(c_{vo}-c_{vi})} = \left[\frac{D}{(\pi t)}\right]^{1/2} \dots(11)$$

If vapor is generated uniformly at a rate m_{vm} at $z = 0$, this mass flux can be expressed in terms of an effective concentration c_{vom} give analogous to equation 6

$$m_v = \frac{D (c_{vom} - c_{vi})}{\left[2\left(\frac{Dt}{\pi}\right)^{1/2}\right]} = \frac{(c_{vom}-c_{vi})\left(\frac{\pi D}{t}\right)^{1/2}}{2} \dots(12)$$

The corresponding effective mass transfer coefficient is defined as

$$h_{Dmt} = \frac{m_{vm}}{(c_{vom}-c_{vi})} = \frac{\left(\frac{\pi D}{t}\right)^{1/2}}{2} \dots(13)$$

It follows from equations 11 and 13 that for the same effective difference in concentration i.e. for

$$(c_{vom} - c_{vi}) = (c_{vo} - c_{vi}) \dots\dots(14)$$

$$\frac{h_{Dmt}}{h_{Dt}} = \frac{\pi}{2} = \frac{h_{Dm}}{h_D}$$

These latter equations are applicable in the region of early developing concentration distribution in a semi-infinite region of air exposed to a water or wet surface. According to Merker for a Rayleigh number $Ra > 1101$, unstable conditions prevail with the result that water vapor is transported upwards away from the wetted surface by means of “thermals” as shown in figure 2.

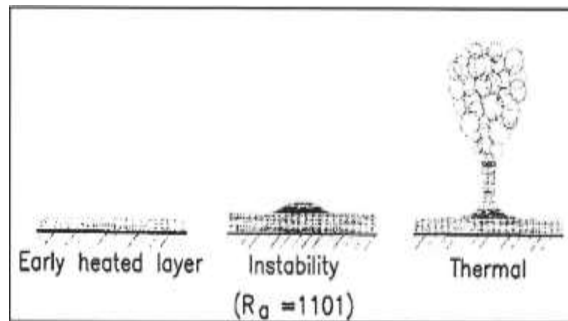


Figure 2. Flow Development Of Air Adjacent To

The generation of such thermals is periodic in time, and both spatial frequency and rate of production are found to increase with an increase in heating rate. For an analysis of the initial developing vapor concentration distribution near the suddenly wetted surface at $z=0$, consider figure 1(a). The approximate magnitude of the curvature of the concentration

Profile is the same as the change in slope $dc_v/\partial z$ across relatively small concentration layer thickness or height δ_D i.e.,

$$\frac{\partial^2 c_v}{\partial z^2} = \frac{\left(\frac{\partial c_v}{\partial z}\right)_{z=\delta_D} - \left(\frac{\partial c_v}{\partial z}\right)_{z=0}}{\delta_D} \dots (15)$$

Figure 1(a) suggests the following concentration gradient scales:

$$\left(\frac{\partial c_v}{\partial z}\right)_{z=\delta_D} = 0$$

$$\left(\frac{\partial c_v}{\partial z}\right)_{z=0} \approx -\frac{(c_{vi} - c_{vo})}{\delta_D}$$

Substitute these gradients into equation 15 and find

$$\frac{\partial^2 c_v}{\partial z^2} \approx -\frac{(c_{vi} - c_{vo})}{\delta_D^2} \dots (16)$$

The approximate magnitude of the term on the right-hand side of equation 1 can be deduced by arguing that the average concentration of the δ_D thick region increases from the initial value c_{vi} by a value of $(c_{vo} - c_{vi})/2$ during the time interval of length t .

$$\frac{\partial c_v}{\partial z} = \frac{c_{vo} - c_{vi}}{(2t)} \dots (17)$$

According to equations 1, 16 and 17 find

$$-\frac{(c_{vi} - c_{vo})}{\delta_D^2} \approx \frac{c_{vo} - c_{vi}}{(2Dt)} \quad \text{Or } \delta_D = (2Dt)^{1/2} \dots (18)$$

The concentration layer becomes unstable when

$$\frac{g \delta_{Du}^3 (\rho_{avo} - \rho_{avi}) c_{p \rho_{av}}}{k \mu} = 1101 \dots (19)$$

Where $\rho_{av} = \frac{(\rho_{avo} + \rho_{avi})}{2}$

At this condition

$$\delta_{Du} = 10.33 \left[\frac{k \mu}{\{g(\rho_{avo} - \rho_{avi}) c_{p \rho_{av}}\}} \right]^{1/3} \dots (20)$$

From equation 18 and 20 find

$$t_u = \frac{53.31 \left[\frac{k \mu}{\{g(\rho_{avo} - \rho_{avi}) c_{p \rho_{av}}\}} \right]^{2/3}}{D} \dots (21)$$

Substitute equation 21 into equation 11 to find

$$h_{Dt} = \frac{\left[\frac{k \mu}{\{g(\rho_{avo} - \rho_{avi}) c_{p \rho_{av}}\}} \right]^{1/3}}{D} = 0.0073 \dots (22)$$

The average mass transfer coefficient during the period r is found by integrating equation 11 i.e.

$$h_D = h_{Dt} = 2 \left[\frac{D}{(\pi t_u)} \right]^{1/2} \dots (23)$$

Or upon substitution of equation 22

If the surface generates vapor at a uniform rate it follows from equation 14 that It is stressed that these equations are only applicable to the first phase of the heat or mass transfer process (growth of concentration layer) and do not include the second phase during which thermals exist (breakdown of concentration layer). No simple analytical approach is possible during this latter phase, although the mean mass transfer coefficient during the breakdown of the concentration layer will probably not differ much from the first phase. This would mean that the mean mass transfer coefficient over the cycle of conduction or concentration layer growth and breakdown is of approximately the same value as that obtained during the first phase of the cycle. By following a procedure similar to the above, the analogous problem of heat transfer during natural convection above a heated horizontal surface for a constant surface temperature of T_0 can be analyzed to find according to Kroger

$$h_T \left[\frac{\mu T}{\{g(T_0 - T_i) c_p \rho^2 k^2\}} \right]^{1/3} = h_T \frac{\left[\frac{k \mu}{\{g(\rho_i - \rho_{av}) c_{p \rho}\}} \right]^{1/3}}{k} = 0.155 \dots (25)$$

And for the case of uniform heat flux q

$$h_q \left[\frac{\mu T}{\{g(T_{0q} - T_i) c_p \rho^2 k^2\}} \right]^{1/3} = h_q \frac{\left[\frac{k \mu}{\{g(\rho_i - \rho_{av}) c_{p \rho}\}} \right]^{1/3}}{k} = 0.243 \dots (26)$$

Where $\rho = \frac{(\rho_o + \rho_i)}{2}$

Note the similarity between equations 23, 24, 25 and 26 respectively. These equations are applicable to natural convection mass and heat transfer respectively. In the absence of winds, effective values of ρ_{avi} in equations 23 and 24 and ρ_i in equation 25 and 26 respectively, change with time ($t > t_u$) during windy periods (forced convection)

evaporation rates generally increase with increasing wind speed. According to the Reynolds-Colburn analogy and the analogy between mass and heat transfer, the following relations exist

$$\frac{h_w Pr^{2/3}}{c_p \rho v_w} = \frac{C_f}{2} = \frac{h_{Dw} Sc^{2/3}}{v_w} \text{ or } h_{Dw} = \frac{C_f v_w}{(2Sc^{2/3})} \dots\dots(27)$$

In general the rate of mass transfer or evaporation from a horizontal wetted surface at a uniform concentration c_{vo} is thus

$$m_{vo} = [h_D + h_{Dw}] (c_{vo} - c_{vi}) \dots\dots(28)$$

Substitute equations 23 and 27 into equation 28 and find

$$m_{vo} = [0.155D \left\{ \frac{g(\rho_{avi} - \rho_{avo})c_p \rho_{av}}{k\mu} \right\}^{1/3} + \frac{C_f v_w}{(2Sc^{2/3})}] (c_{vo} - c_{vi})$$

$$m_{vo} = \left[\frac{0.155 \left\{ \frac{g\mu^2(\rho_{avi} - \rho_{avo})c_p}{(k\rho_{av}^2)} \right\}^{1/3}}{Sc} + \left(\frac{C_f v_w}{2Sc^{2/3}} \right) \right] (c_{vo} - c_{vi}) \quad (29)$$

For relatively small temperature differences, the concentrations in equation 29 can be replaced by the partial vapor pressures i.e. $c_v = p_v/R_v T_{oi}$, where $T_{oi} = (T_o + T_i)/2$ and $R_v = 461.52 \text{ J/Kg K}$ Furthermore, for air-water vapor mixtures $Sc = 0.6$.

Substitute these values into equation 29 and find

$$m_{vo} = 5.6 \times 10^{-4} \left[\frac{g\mu^2(\rho_{avi} - \rho_{avo})c_p}{(k\rho_{av}^2)} \right]^{1/3} + 2.72C_f v_w \left] \frac{(p_{vo} - p_{vi})}{T_{oi}} \dots(30)$$

Similarly, if the vapor is generated uniformly at $z = 0$ find the rate of evaporation according to equations 24, 27 and 28 i.e.

$$m_{vo} = 8.78 \times 10^{-4} \left[\frac{g\mu^2(\rho_{avi} - \rho_{avo})c_p}{(k\rho_{av}^2)} \right]^{1/3} + 1.735C_f v_w \left] \frac{(p_{vo} - p_{vi})}{T_{oi}} \dots(31)$$

Since the thermal conductivity of water is not negligible, it is not possible to achieve a truly uniform heat flux situation. The value of the dimensionless mass transfer coefficient as given by equation 24 may thus be less than 0.243, i.e. it will be some value between 0.243 and 0.155 as given by equation 23. Burger and Kroger report the results of experiments conducted during analogous heat transfer tests between a low thermal conductivity horizontal surface and the environment. They obtain a value of 0.2106 instead of the theoretical value of 0.243 given in equation 26 and the analogous equation 24. They furthermore obtain a value of $C_f = 0.0052$ based on a wind speed measured 1 m above the test surface. With these values equation 26 applied over a wetted surface can be extended to become

$$h_q \left\{ \frac{\mu}{g c_p \rho_{av} k^2 (\rho_{avi} - \rho_{avo})} \right\}^{1/3} = 0.2106 + 0.0026 v_w \left[\frac{\rho_{av}^2}{g\mu^2 (\rho_{avi} - \rho_{avo})} \right]^{1/3} \dots\dots(32)$$

When density differences are very small and conditions near the surface are relatively stable or at night when $T_{oq} < T_i$, and the heat flux is uniform they recommend

$$h_q = 3.87 + \frac{0.022 c_p \rho_{av} v_w}{\left(\frac{\mu c_p}{k} \right)^{2/3}} \dots\dots(33)$$

In cases where $T_{oq} < T_i$ and h_q according to equation 33 is larger than the value of h_q , obtained according to equation 32, the former is applicable. If the above values (0.2106 and

$C_f = 0.0052$) are substituted into equation 31 find

$$m_{vo} = 7.61 \times 10^{-4} \left[\left\{ \frac{g\mu^2(\rho_{avi} - \rho_{avo})c_p}{(k\rho_{av}^2)} \right\}^{1/3} + 0.0104 v_w \right] \frac{(p_{vo} - p_{vi})}{T_{oi}} \dots\dots(34)$$

A mass transfer coefficient that is analogous to equation 33 is given by

$$h_{Dm} = \frac{h_q}{\rho_{av} c_p} \left(\frac{Pr}{Sc} \right)^{2/3} = \frac{3.87}{\rho_{av} c_p} \left(\frac{Pr}{Sc} \right)^{2/3} + \frac{0.0022 v_w}{Sc^{2/3}} \dots\dots(35)$$

The corresponding uniform mass transfer rate is

$$m_{vom} = \left[\frac{3.87}{\rho_{av} c_p} \left(\frac{Pr}{Sc} \right)^{2/3} + \frac{0.0022 v_w}{Sc^{2/3}} \right] \frac{(p_{vo} - p_{vi})}{T_{oi}} \dots\dots(36)$$

For $Sc = 0.6$, $Pr = 0.7$ and $R_v = 461.52 \text{ J/kg K}$ find

$$m_{vom} \approx \left[\frac{0.0093}{(\rho_{av} c_p)} + 6.7 \times 10^{-4} v_w \right] \frac{(p_{vo} - p_{vi})}{T_{oi}} \dots(37)$$

Equation 37 is found to be in good agreement with equations recommended by Tang et al.a. This expression is applicable at night and during the day when the value m_{vom} is found to be larger than that given by equation 34. The density of the ambient air is given by

$$\rho_{\text{av}} = (1 + w_i) \left[1 - \frac{w_i}{w_i + 0.622} \right] \frac{p_a}{287.08T_i} \quad \dots(38)$$

Where p_o is the pressure and T_i is the temperature of the ambient air. If the relative humidity of the ambient is known

$$\Phi = \frac{P_{\text{vi}}}{P_{\text{vsi}}} \quad \dots(39)$$

The vapor pressure in the air can be expressed as

$$P_{\text{vi}} = \Phi P_{\text{vsi}} \approx \Phi \times 2.368745 \times 10^{11} \exp\left(-\frac{5406.1915}{T_i}\right) \quad (40)$$

The humidity ratio of the ambient air is given by

$$w_i = \frac{0.622P_{\text{vi}}}{P_a - P_{\text{vi}}} \quad \dots(41)$$

Similarly the density of the saturated air at the surface of the water is

$$\rho_{\text{av}} = (1 + w_o) \left[1 - \frac{w_o}{w_o + 0.622} \right] \frac{p_a}{287.08T_o} \quad \dots(42)$$

Where

$$w_o = \frac{0.622P_{\text{vo}}}{P_a - P_{\text{vo}}} \quad \dots(43)$$

And

$$P_{\text{vo}} \approx 2.368745 \times 10^{11} \exp\left(-\frac{5406.1915}{T_o}\right) \quad (44)$$

By applying an energy balance to the surface of film of water on a plate that is exposed to the natural environment, it is possible to obtain an expression for the rate of evaporation per unit surface area i.e.

$$m_{\text{en}} = \frac{[\alpha_h - \epsilon_w \sigma (T_{\text{sq}}^4 - T_{\text{sky}}^4) - h_q (T_{\text{sq}} - T_i)]}{h_{\text{fg}}} \quad (45)$$

Where α_h represents the solar radiation absorbed by the surface, $\epsilon_w \sigma (T_{\text{sq}}^4 - T_{\text{sky}}^4)$ is the sky radiation while $h_q (T_{\text{sq}} - T_i)$ is the convective heat transfer rate. The absorptivity of solar radiation at the surface of the water is given by Holman and can be approximated by the following equation.

$$\alpha_w = 0.989 - \frac{2.05}{(90 - \theta_z)} \quad (46)$$

Where θ_z is the zenith angle measured in degrees. The surface emits radiation to a sky temperature T_{sky} which can be calculated according to

$$T_{\text{sky}} = \epsilon_{\text{sky}}^{\frac{1}{4}} T_o \quad \dots(47)$$

Berdahl and from berg express the emissivity of the sky ϵ_{sky} During the day as

$$\epsilon_{\text{sky}} = 0.727 + 0.0060 T_{\text{dp}} \quad \dots(48)$$

during the day as

$$\epsilon_{\text{sky}} = 0.741 + 0.0062 T_{\text{dp}} \quad \dots(49)$$

Where T_{dp} is the dew-point temperature measured in degrees Celsius. The heat transfer coefficient h_q is given by equation 32 while equation 33 is applicable when $T_{\text{sq}} > T_i$ or when the value of h_q , according to equation 33 during the day is larger than the value obtained according to equation 32. The heat transfer through the plate is negligible. According to Holman the intensity of solar radiation in clear water at a distance z from the surface is given by

$$I_z = 0.6 I_h e^{-0.16z} \quad \dots(50)$$

For a thin film of thickness $z = 0.0015$ m the heat flux near the surface of the film is thus approximately

$$k \frac{dT}{dz} = I_z = 0.6 I_h \quad \dots(51)$$

or the surface temperature can be described by

$$T_{\text{oq}} = T_{\text{o measured}} - \frac{0.6 I_h z}{k} = T_{\text{o measured}} - 0.0015 I_h \quad \dots(52)$$

EXPERIMENTAL ANALYSIS

Test set up contains basically six components viz. Effluent, bottom tank, overhead tank, plate, frame, pumping system. Bottom tank and overhead tanks having same dimension of 1068×300×300 mm made of thin gauge coated steel sheet are manufactured from the “Super cooler services” Plate is made of coated steel sheet which is bend from the nearby factory in M.I.D.C. Plate have dimension after bending 1068×2500 mm. Frame is made of 1 inch L-section. Frame is fabricated in “Essential equipment “in dhule M.I.D.C. Pump of 35Watts of discharge height of

2.4M. with LDPE pipe of length approx 12feet purchased from “ Super cooler services”. Project is assembled in the “Essential equipment” testing procedure is under trail with some reliable observation and result.



Experimental test set up

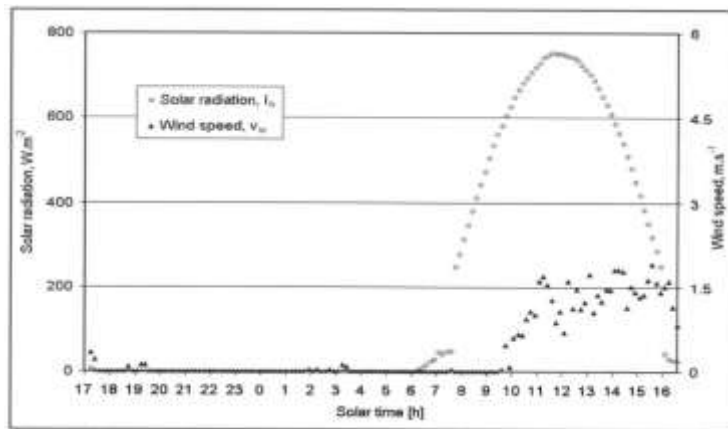
RESULTS

	Time	Air vel. M/s	RH (%)	DBT (°C)	WBT (°C)
Inlet	12 P.M.	2	10.7	49.5	22.3
Outlet		2	11.3	46.4	23.2
Inlet	1 P.M.	1.2	14	47.4	22.6
Outlet		1.2	13	45.2	20.8
Inlet	2 P.M.	1	12.5	46.6	19.8
Outlet		1	14	45.2	20.5
Inlet	3 P.M.	1.2	13	41.1	19.6
Outlet		1.2	14	40.8	20.2
Inlet	4 P.M.	1.1	12	39.9	19.6
Outlet		1.1	13	38.6	20
Inlet	5 P.M.	1.2	14.4	37.8	18.8
Outlet		1.2	14	37.2	18.9

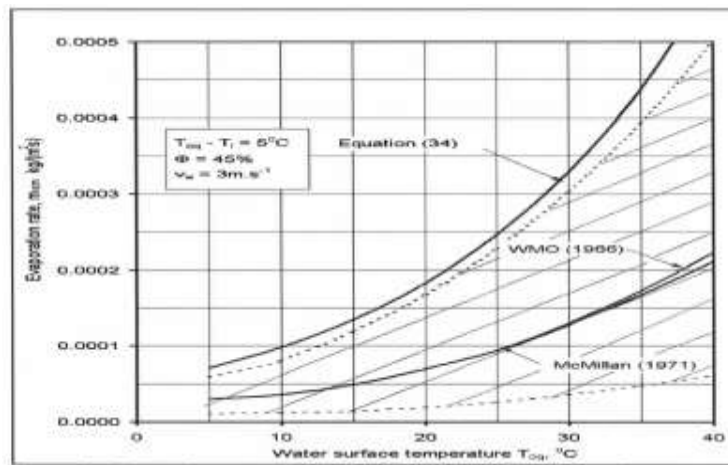
	Time	water Temp (°C)	R (Nor.) W/m ²	R (Hor.) W/m ²	Mass of system
Inlet	12 P.M.	35	1015	1010	45.55
Outlet					
Inlet	1 P.M.	35	965	920	
Outlet					
Inlet	2 P.M.	34.5	910	805	
Outlet					
Inlet	3 P.M.	34	850	725	
Outlet					
Inlet	4 P.M.	34	702	655	
Outlet					
Inlet	5 P.M.	33	445	385	32.05

Comparative study between normal, horizontal and projected surfaces

	Total mass transfer	Mass per second	Rad. on surface	Gain
Inclined surface	13.4	7.44×10^{-4}	965	54.64%
Hor. surface	8.65	4.80×10^{-4}	702	-
Proj. surface	7.46	4.16×10^{-4}	702	-



Effect of Air Velocity, Solar Radiation, Time Of Day



Effect of Water Temperature on Evaporation

CONCLUSION

The evaporation rate of water in the effluent increases, due to increase in aperture area, wind speed and due to decrease in relative humidity and mass flow rate. The performance of the experimental analysis is varying 12% in comparison with that of the theoretical analysis. From these results of the theoretical and experimental satisfying the performances of test setup. This system improves the evaporation rate by comparing the Horizontal surface and Projected surface area with respect to inclined surface

REFERENCES

1. K. Srithar, A. Mani “Analysis of a single cover FRP flat plate collector for treating tannery effluent” *Applied Thermal Engineering* 24 (2004) 873–883 .
2. Soteris A. Kalogirou “Flat-plate collector construction and system configuration to optimize the thermosiphonic effect *Renewable Energy* 67 (2014) 202-206.
3. Omid Mahian a, Ali Kianifar a, Soteris A. Kalogirou b, Ioan Pop c, Somchai Wongwises “A review of the applications of nanofluids in solar energy” *International Journal of Heat and Mass Transfer* 57 (2013) 582–594 .
4. Jia Liu a,b, Haisheng Chen a,* , Yujie Xu a, Liang Wang a, Chunqing Tan a “A solar energy storage and power generation system based on supercritical carbon dioxide” *Renewable Energy* 64 (2014) 43-51.
5. Hossein Taghvaei a, Hamed Taghvaei b, Khosrow Jafarpur a, M.R. Karimi Estahbanati c, Mehrzad Feilizadeh c, Mansoor Feilizadeh b, A. Seddigh Ardekani b “A thorough investigation of the effects of water depth on the performance of active solar stills” *Desalination* 347 (2014) 77–85.
6. M.A. Minn a, K.C. Ng a,* , W.H. Khong b, T. Melvin “A distributed model for a tedlar-foil flat plate solar collector” *Renewable Energy* 27 (2002) 507–523.
7. S. Santoyo-Guti rreza,* , J. Siqueirosb, C.L. Heardc, E. Santoyod, F.A. Hollande “An experimental integrated absorption heat pump effluent purification system. Part II: operating on water/Carrol solutions” *Applied Thermal Engineering* 20 (2000) 269-284.
8. T. Rajaseenivasan, P. Nelson Raja, K. Srithar, “An experimental investigation on a solar still with an integrated flat plate collector” *Desalination* 347 (2014) 131–137 .
9. K. Srithar, A. Mani “Analysis of a single cover FRP flat plate collector for treating tannery effluent” *Applied Thermal Engineering* 24 (2004) 873–883
10. H.O. Njokua* and O.V. Ekechukwub. “Analysis of the exergetic performance of the reverse-side absorber-plate shallow solar pond” *International Journal of Sustainable Energy* Vol. 30, No. 6, December 2011, 336–352.
11. Sartori, E, A critical review on equations employed for the calculation of the evaporation rate from free water surfaces, *Solar Energy*,2000, 68(1),77-89.
12. Srithar K.(Srithar,2010), “Performance Analysis of Vapour Adsorption Solar Still Integrated with Mini-solar Pond for Effluent Treatment”, vol. 1,no. 4,December 2010; ISSN: 2010-0221.
13. T. Rajaseenivasan a, P. Nelson Raja a, K. Srithar “ An experimental investigation on a solar still with an integrated flat plate collector” *Desalination* 347 (2014) 131–137.
14. K. Kalidasa Murugavela, Kn.K.S.K. Chockalingama, K. Srithar “An experimental study on single basin double slope simulation solar still with thin layer of water in the basin *Desalination* 220 (2008) 687–693.